

***In vivo* visualisation by three-dimensional optical coherence tomography of stress crazing of a bioresorbable vascular scaffold implanted for treatment of human coronary stenosis**

Maria D. Radu¹, MD, Yoshinobu Onuma¹, MD, Richard J. Rapoza², PhD, Roberto Diletti¹, MD, Patrick W. Serruys^{1*}, MD, PhD

1. Thoraxcenter, Erasmus MC, Rotterdam, The Netherlands; 2. Abbott Vascular, Santa Clara, CA, USA

The concept of using bioresorbable intracoronary scaffolds in percutaneous coronary intervention has attracted interest since their inception, because these devices can overcome potential disadvantages of permanent metallic stents. The bioresorbable vascular scaffold (BVS) (Abbott Vascular, Santa Clara, CA, USA) has a bioresorbable polymer backbone of poly-L-lactide (PLLA) coated with the polymer poly-D,L-lactide (PDLLA) that contains and controls the release of the antiproliferative drug, everolimus. Both PLLA and PDLLA are fully bioresorbable. The BVS backbone is laser cut from a cylinder of polymer, resulting in a scaffold composed of a number of in-phase zigzag hoops linked together by three longitudinal bridges (**Figure 1**). After having been cut, the scaffold is crimped onto a balloon. During the crimping process, hinge points of the scaffold are subject to significant deformation, both in tension and compression. This deformation beyond the yield point can induce crazing of the polymer. When a polymer crazes, it absorbs the energy of the deformation by creating new surfaces; leading to an increase in the material's toughness.¹ This crazed material still supports mechanical loads and deformation.

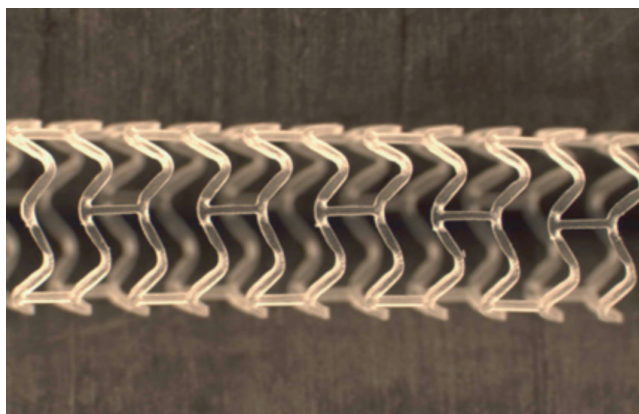


Figure 1. Design of the BVS scaffold.

Crazing of the polymer induces a change in its light transmission by increasing scattering at the newly created interfaces, which in turn reflect light intensely (**Figure 2A**).

*Corresponding author: Thorax Center, Erasmus MC, 's Gravendijkwaal 230, 3015 Rotterdam, The Netherlands
E-mail: p.w.j.c.serruys@erasmusmc.nl

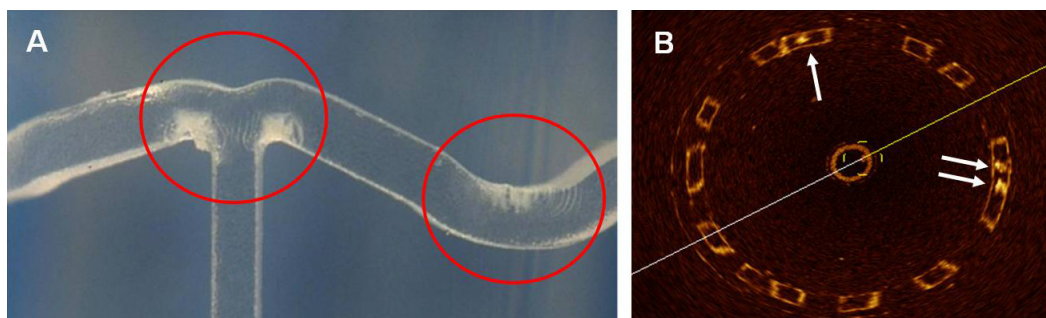


Figure 2. Macroscopic and OCT identification of changes in the transparency by applying strain to the polymer. A) Macroscopic examination of the BVS. Red rings indicate the white strained points. B) OCT *in vitro* has shown that these are visualised as struts where the dark centres contain nuclei of high signal-intensity surrounded by dark transparent material (arrows). The remaining struts have bright borders with dark centres.

Analysis of the scaffold by the finite element method (FEM) suggests that the maximum amount of stress in the crimped state of the BVS is located near the outer surface of the zigzag curvature, while the maximum amount of stress is located near the inner surface of the curvature (**Figure 3**). Inspection of the BVS with scanning electron microscopy (SEM) has shown that small cone-shaped cavities form at the inner parts of the curvatures, perhaps due to micro-separation of the polymer lamellae in the high stress regions after deployment. Another consequence of the crimping process is the “lifting” and “depression” seen at the scaffold surface (**Figure 4**) around the hinge points in the polymer scaffold.

Optical coherence tomography (OCT) is an infrared light-based imaging technique with the highest resolution ($\sim 10 \mu\text{m}$) available for *in vivo* use to date. Since the BVS polymer is translucent, it is visualised by OCT to a greater extent than metallic stents, in that the abluminal boundary of struts is also visible. As crazing reflects light intensely, the resulting scattering centres are identified by OCT as nuclei of a high signal-intensity surrounded by dark transparent material (**Figure 2B**).

We present an example of a BVS implanted *in vivo* in a human coronary artery imaged with OCT immediately after implantation.

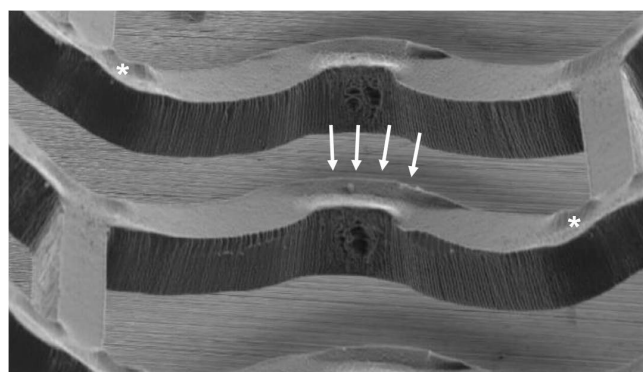


Figure 4. Scanning electron microscopy of the BVS. Arrows and asterisks indicate “lifting” and “depression” of the BVS surface, respectively.

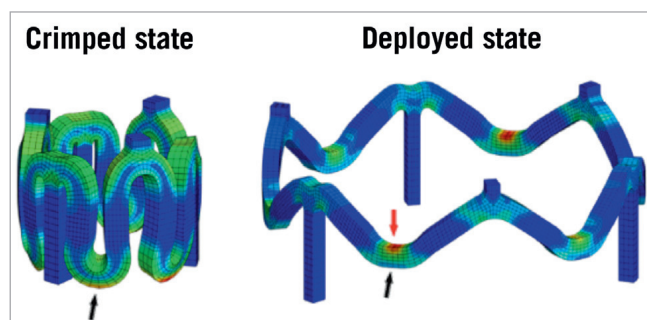


Figure 3. Finite element analysis of the amount of stress in the BVS. Blue and red colours indicate the minimum and maximum amount of stress, respectively. Black arrows: outer surface of curvature; red arrow: inner surface of curvature.

Images were acquired with the C7-XR system (LightLab Imaging, Westford, MA, USA) at a frame rate of 100 frames/s, and pullback speed of 20 mm/s. By analysis of 89 consecutive frames, we found 552 struts with bright borders and dark centres, and 56 struts also containing scattering centres. For visualisation of the location of the latter, we performed a three-dimensional (3D) reconstruction of the scaffold with separate colour-coding of the two strut types, using the Analyze 9.0 software (Analyze Direct, Overland Park, KS, USA). **Figure 5** demonstrates that struts containing scattering centres are *in vivo* located at the curvatures of the scaffold, where the highest strains are experienced during crimping and deployment. In the 3D reconstruction, the crazing does not appear to be systematically present at all curvatures. This could be related to factors such as the underlying plaque type or malapposition, but is more likely due to the relatively low frame rate and fast pullback speed of OCT, causing some of the stressed points to remain undetected.

A type of strain similar to the one described here for the BVS, likely occurs in metallic stents as well, but since the OCT light cannot penetrate metal², it has not been possible to study this phenomenon *in vivo* previously. Clinical data thus far have indicated that the BVS is safe.^{3,4} However, although very rare, structural

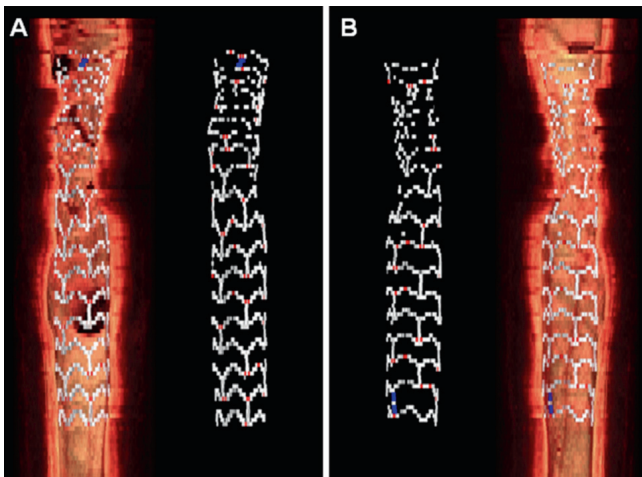


Figure 5. Three-dimensional reconstruction of OCT acquisition of the BVS. The BVS is depicted from the front (A) and back (B), with and without the underlying vessel wall. The point of stress crazing is indicated with red, and the platinum marker with blue. The design pattern in the proximal (top) part of the BVS is distorted due to cardiac motion.

discontinuities related to overstretching of the scaffold beyond certain diameters during deployment, accompanied by clinical symptoms, have been reported recently.^{4,5} Whether there may be a relationship between the crazing in the BVS, as visualised with OCT, and structural discontinuities, is not yet known.

In conclusion, correlation of the location of high strain areas, cone-shaped cavities, and scattering centres by FEM, SEM, macroscopic examination, and 3D OCT, respectively, together suggest that OCT can visualise the point of stress crazing in the BVS

in vivo, and may thus be applied in the study of similar length scale changes in material characteristics over the lifetime of bioresorbable vascular scaffolds.

Conflict of interest

Richard J. Rapoza is an employee of Abbott Vascular. The other authors have no conflict of interest to declare.

References

1. American Society of Metals. Characterization and Failure Analysis of Plastics. *ASM International* 2003;204-210.
2. Serruys PW, Ormiston JA, Onuma Y, Regar E, Gonzalo N, Garcia-Garcia HM, Nieman K, Bruining N, Dorange C, Miquel-Hébert K, Veldhof S, Webster M, Thuesen L, Dudek D. A bioabsorbable everolimus-eluting coronary stent system (ABSORB): 2-year outcomes and results from multiple imaging methods. *Lancet* 2009;373:897-910.
3. Radu M, Jørgensen E, Kelbaek H, Helqvist S, Skovgaard L, Saunamäki K. Strut apposition after coronary stent implantation visualised with optical coherence tomography. *EuroIntervention* 2010;6:86-93.
4. Onuma Y, Serruys PW, Ormiston JA, Regar E, Webster M, Thuesen L, Dudek D, Veldhof S, Rapoza R. Three-year results of clinical follow-up after a bioresorbable everolimus-eluting scaffold in patients with de novo coronary artery disease: the ABSORB trial. *EuroIntervention* 2010;6:447-453.
5. Serruys PW, Onuma Y, Ormiston JA, de Bruyne B, Regar E, Dudek D, Thuesen L, Smits PC, Chevalier B, McClean D, Koolen J, Windecker S, Whitbourn R, Meredith I, Dorange C, Veldhof S, Miquel-Hébert K, Rapoza R, Garcia-Garcia HM. Evaluation of the second generation of a bioresorbable everolimus drug-eluting vascular scaffold for treatment of de novo coronary artery stenosis: six-month clinical and imaging outcomes. *Circulation* 2010;122:2301-2312.